International Journal of Engineering & Technology, 7 (4.30) (2018) 334-337

SPC

International Journal of Engineering & Technology

Website: www.sciencepubco.com/index.php/IJET

Research paper



Graphite Saturable Absorber for Q-Switched Fiber Laser

Yushazlina R. Yuzaile[1], *Noor A. Awang[1], Zahariah Zakaria[1], Noor U.H.H Zalkepali[1], Amirah A. Latif[2], Atiqah N. Azmi[1] and Fatin S. Abdul Hadi[1]

[1]Optical Fiber Laser Technology (OpFLAT) Focus Group, Department of Physics and Chemistry, Faculty of Applied Sciences and Technology, Universiti Tun Hussein Onn Malaysia, 84600, Pagoh, Johor, Malaysia.
[2]Department of Physics, Faculty of Science, Universiti Putra Malaysia, Selangor, Malaysia.
**Corresponding author E-mail: norazura@uthm.edu.my*

Abstract

This paper reported a successful demonstration on Q-switched fiber laser by using graphite as saturable absorber (SA). The graphite is deposited on the fiber ferrule through a simple mechanical exfoliation method. The modulation depth of the graphite SA is 19.2% with a saturation intensity of 85 MW/cm². The maximum achievable pulse repetition rates and pulse width are 42.41 kHz and 3.40 µs respectively. Meanwhile, its optical signal-to-noise ratio is about 50.81 dB. The Q-switched pulses have the maximum pulse energy of 5.84 nJ. These outcomes demonstrated that a stable output of passively Q-switched fiber laser is produced and can be applied for various optical fiber applications.

Keywords: *Graphite; Mechanical Exfoliation; Q-Switching; Q-Switched Fiber Laser; Saturable Absorber*

1. Introduction

Recently, Q-switched fiber laser has been implemented in various applications including communication, medical, industrial processing, remote sensing and military [1-6]. This pulsed fiber laser source has attracted a huge technical attention due to its uncomplicated configuration and easy operation. Besides, it has numerous advantages including alignment-free operation, low heat accumulation, high beam quality and compactness [7]. Besides that, Q-switching is applicable in two ways which are active and passive. A passively Q-switching technique uses a saturable absorber (SA) to modulate the intracavity losses which result in a high energy pulse [8]. Semiconductor saturable absorber mirrors (SESAMs) have been commonly used in producing the Q-switching pulses but the performance is limited by the operating wavelength. Besides, the high fabrication cost is one of the issues too [9]. Hence, other alternatives were being investigated until the carbon nanotube (CNT) SA was found later. The CNT SAs have been widely implemented for Q-switching and mode-locking at different operating wavelengths [10-11].

In 2009, Bao et al. [12] had reported the first effective graphene saturable absorber, comprising a broadband operating bandwidth. Since then, graphene-based SA has been extensively investigated for passively Q-switching and mode-locking since graphene has a with zero band gap semiconducting feature. Recent researches have reported many alternatives for the saturable absorption materials such as the transition metal dichalcogenides (TMDs) and the topological insulators (TIs), for instance, bismuth selenide (Bi_2Se_3) [13-14], molybdenum disulphide (MoS_2) [15], molybdenum selenide ($MoSe_2$) [16] and tungsten disulphide (WS_2) [17]. Metal nanoparticles such as gold and silver based SAs are also the excellent candidates [18-19].

Nevertheless, graphene is still the most favourable SA as it has the ultimate potentials for the implementation of the efficient pulsed fiber lasers and solid-state lasers [20-25]. However, there is a critical aspect that is essentially required for the realization of a practical graphene SA, which is its material structure. Both of the crystalline-structured and few-layered graphene SAs are fabricated by the complex and sophisticated fabrication methods such as chemical vapour deposition (CVD) [26], pulsed-laser deposition (PLD) [27] and chemical synthesis [28-30]. Therefore, some possible alternatives such as graphite and graphene oxide are introduced.

Graphite [31-35] and graphene oxide [36-40] are the carbon-based materials that provide comparable saturable-absorption properties to few-layered graphene, which can serve as a cost-effective and practical SA despite the relatively low crystalline quality. Only a few studies on graphite-based SA have been reported to date [31-35]. The previous works used graphite nanoparticles that were prepared through the mechanical-trituration process [32], electrochemical exfoliation [34], PVA-brushing/nanoparticle imprinting [31] and the aqueous nanoparticle-solution-dropping method [35]. A much simpler fabrication method is presented in this paper to fabricate the graphite SA in which the SA is prepared by using graphite flakes which are commercially available.

2. Experimental Details

2.1. Preparation and characterization of graphite SA

The fabrication process begins with the preparation of the SA material. The commercial natural graphite flakes (obtained from HQ Graphene) are used as the base material for the SA preparation. The flakes are transferred onto a scotch tape to prepare for the exfoliation process. The fiber ferrule is first cleaned with isopropyl alcohol and then pressed onto the graphite flakes as shown in Figure 1. Figure 2 shows the graphite on the fiber ferrule's surface after being mechanically exfoliated.

Copyright © 2018 Authors. This is an open access article distributed under the Creative Commons Attribution License, which permits unrestricted use, distribution, and reproduction in any medium, provided the original work is properly cited.

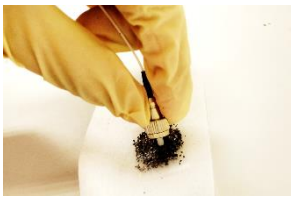

Fig. 1: Exfoliating the graphite flakes on fiber ferrule

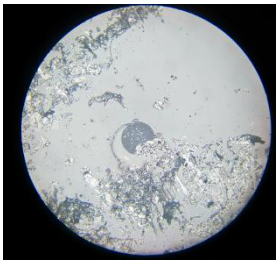

Fig. 2: Graphite under the fiberscope

The morphology and the elemental analysis of the graphite SA are inspected by the scanning electron microscope (SEM, FEI) and the energy dispersive spectroscopy (EDS, Aztec Energy). Figure 3 shows the graphite image after being scanned by the SEM. The EDS analysis clearly shows the composition of graphite with a strong intensity peak of carbon (C) element as in Figure 4. The presence of the silicon (Si) and oxygen (O) elements are due to the fiber (silica, SiO_2) detected by the EDS.

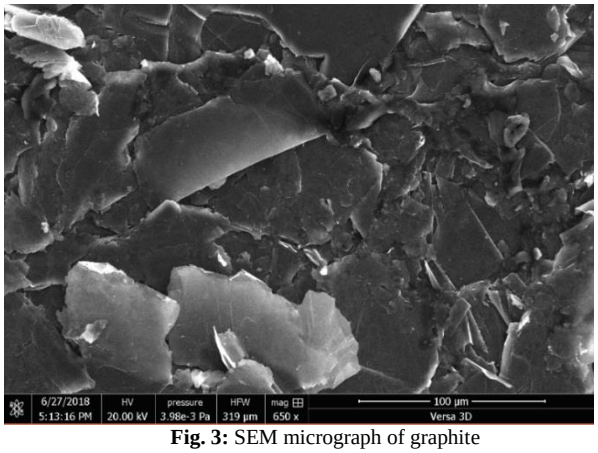

Fig. 3: SEM micrograph of graphite

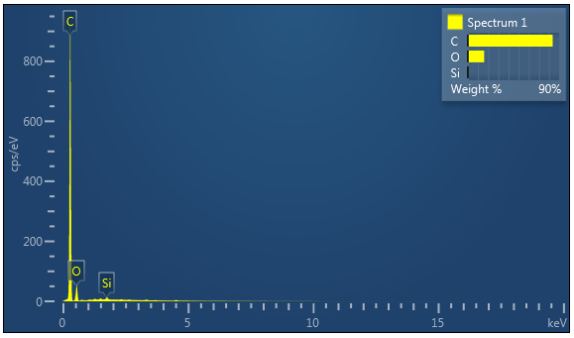

Fig. 4: EDS analysis on graphite SA

2.2. Measuring the modulation depth of graphite SA

A balanced twin detector method is applied for measuring the modulation depth (saturable absorption) of the graphite SA. The method is based on a pulsed fiber laser source with a central wavelength and a pulse repetition rate of 1558 nm and 2.833 MHz respectively. The setup for the measurement is illustrated in Figure 5. Two optical power meters are used to measure two output signals (Path 1 & Path 2). Path 1 is set for the reference power measurement while Path 2 for power absorption measurement. The measured modulation depth of the graphite SA is 19.2% with a saturation intensity of 85.0 MW/cm², shown in Figure 6. As the intensity beam increases, the absorbance decreases to indicate the possibility of a passive amplitude modulation of the incident beam with simple laser device [42]. The typical nonlinear absorbance formula is expressed by Equation 1 [41].

$$\alpha(I)=\frac{\alpha_s}{1+\frac{I}{I_s}}+\alpha_{ns} \quad (1)$$

Definition 2.1: *$\alpha(I)$ indicates the absorption coefficient, α_s and α_{ns} are the saturable losses and non-saturable losses respectively, I is the intensity of the laser light and I_s is saturation intensity.*

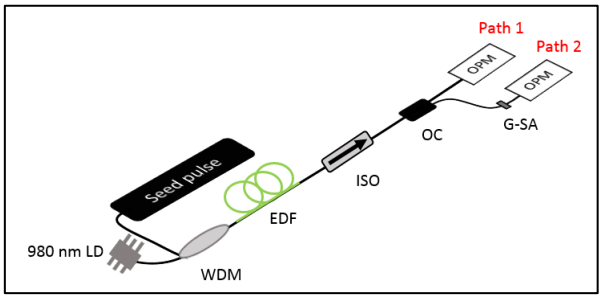

Fig. 5: Twin detector method

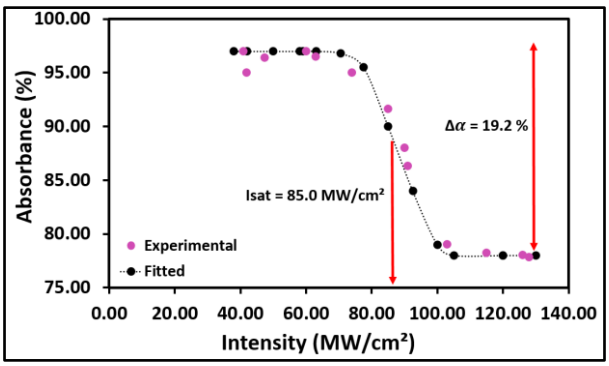

Fig. 6: The modulation depth of graphite SA

2.3. Experimental setup

The Q-switched fiber laser is set up experimentally as shown in Figure 7. A 5 m erbium-doped fiber (EDF) with the absorption coefficient of 5.09 dB/m at 979 nm of wavelength is used as an active medium. The EDF is pumped by a 980 nm Oclaro LC 96A74P-20R laser diode through a 980/1550 nm of wavelength division multiplexer (WDM). To ensure a unidirectional light propagation, an isolator (ISO) is placed right after the EDF. Meanwhile, the graphite SA (G-SA) is employed in between the isolator and the polarization controller (PC). The output is analyzed by the optical spectrum analyzer (OSA) and the oscilloscope (OSC) via 90:10 optical coupler, connected to a 50:50 optical coupler. The overall cavity length is about 15 m.

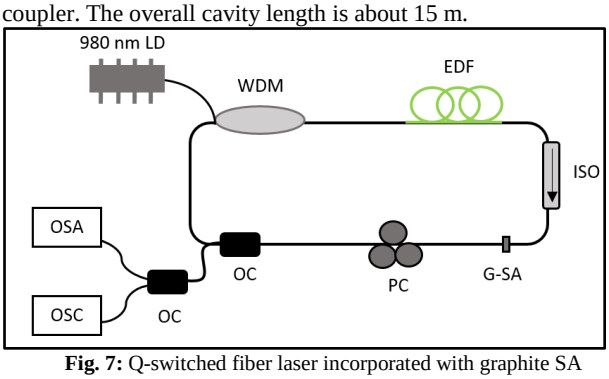

Fig. 7: Q-switched fiber laser incorporated with graphite SA

3. Results and Discussions

The output spectra are observed as increasing the pump power. The Q-switching started at the threshold pump power of 15.9 mW. They are stable until reaching the maximum pump power of 95.4 mW. By referring to Figure 8, the solid line shows the Q-switched emission spectrum with a central wavelength and a 3 dB bandwidth of 1558 nm and 2.92 nm respectively. It can be clearly seen that the Q-switched spectrum has a broader bandwidth than the continuous wave spectrum (dashed line) which occurred as a large population inversion is achieved, producing a single short laser pulse. Also, it is caused by the large normal dispersion of the fiber cavity.

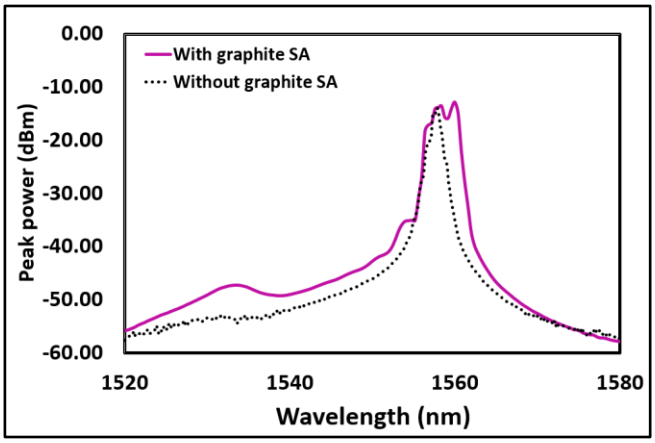

Fig. 8: Output optical spectra at 95.4 mW of pump power

Figure 9 indicates the pulse trains extracted from the oscilloscope at 95.4 mW of pump power, via a 5 GHz bandwidth photodetector. The time interval and the constant peak intensity are 23.58 µs and 0.25 V, respectively which corresponds to a repetition rate of 42.41 kHz, with a pulse width of 3.40 µs.

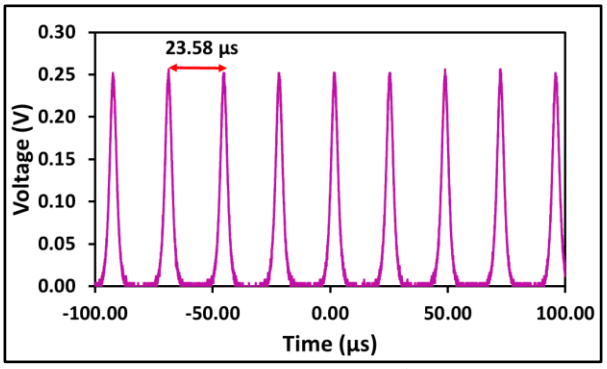

Fig. 9: Pulse train at 95.4 mW of pump power

The relationship between the repetition rate, pulse width and pulse energy is shown in Figure 10. The repetition rate shows a linear increment from 15.20 kHz to 42.41 kHz. Meanwhile, the pulse width decreased linearly from 8.68 µs to 3.4 µs. These trends prove the typical characteristics of Q-switching operation [18].

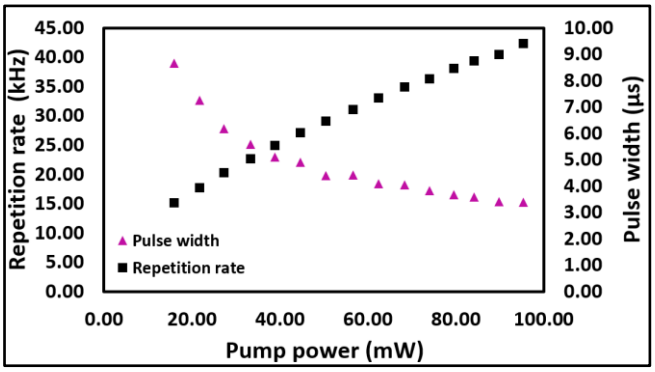

Fig. 10: Pulse repetition rate and pulse width versus pump power

Figure 11 shows the peak power and energy variations of the generated pulse. At the maximum pump power, the pulse energy and the peak power are 5.84 nJ and 0.25 mW respectively. Both of the parameters are increased in correspondence with the increase of the latter. Besides, it can be seen that both parameters are a near-inverse match to the pulse width.

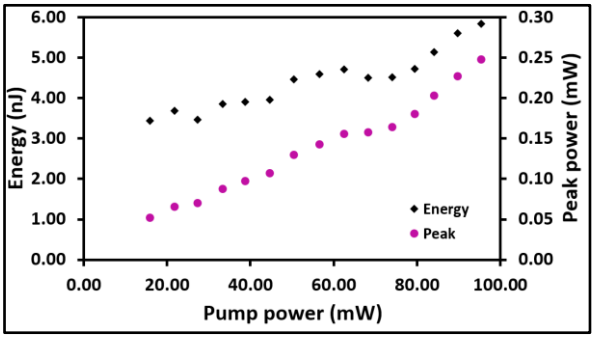

Fig. 11: Pulse energy and peak power variations

The radio frequency (RF) spectrum is shown in Figure 12, taken at the maximum pump power of 95.4 mW, with 30 Hz of resolution bandwidth. The fundamental frequency of the spectrum was 42.41 kHz with a signal-to-noise ratio (SNR) of 50.81 dB.

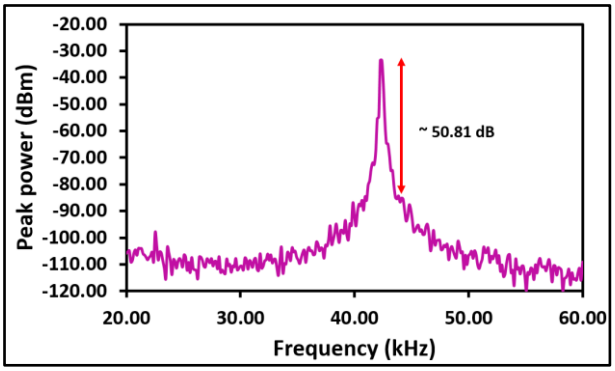

Fig. 12: RF spectrum at the maximum pump power of 95.4 mW

Table 1 shows the performance comparison between the graphite-based SA in this work with the previous researches. Although the modulation depth in this work is quite small, however, it is sufficiently enough to realize Q-switching.

Table 1: Graphite-based SAs and their pulse parameters

Graphite-based SA fabrication techniques	Modulation depth (%)	Repetition rates	Pulse width	References
PVA-brushing/nanoparticle imprinting	20.0	7.00 MHz	1.20 ps	[31]
Mechanical-trituration	54.0	9.10 MHz	1.67 ps	[32]
Electrochemical exfoliation	53.0	30.61 MHz	430 fs	[34]
Aqueous nanoparticles-solution dropping	55.0	1.26 THz	335 fs	[35]
Pencil sketching	1.0	46.08 kHz	1.98 µs	[33]
Simple mechanical exfoliation	19.2	42.41 kHz	3.40 µs	This work

4. Conclusion

A simple and easy preparation method of the graphite-based SA has been successfully demonstrated in this paper. The results and the performance of the prepared SA are comparable for a passively Q-switched fiber laser. It is believed that this SA has a huge potential as a practical and efficient SA in the ultrafast photonics.

Acknowledgement

Authors sincerely thank Research Management Centre (RMC) of Universiti Tun Hussein Onn Malaysia for providing the funding for this work under the Postgraduate Research Grant GPPS: H065 and TIER 1 Grant: H133.

References

[1] Ahmad H, Awang NA, Paul MC, Pal M, Latif AA & Harun SW (2012), All fiber passively mode locked zirconium-based erbium-doped fiber laser. *Optics & Laser Technology* 44, 534-537.

[2] Shang L, Ning J & Yang X (2012), An experimental study of an acousto-optic q-switched yb^{3+}-doped all-fiber laser *Optik* 123, 1061-1062.

[3] Gaponenko MS, Onushchenko AA, Kisel VE, Malyaevich AM, Yumashev KV & Kuleshov NV (2012), Compact passively q-switched diode-pumped tm:ky$(wo^4)_2$ laser with 8 ns/30 μJ pulses. *Laser Physics Letters* 9, 291-294.

[4] Kurkov AS, Sadovnikov YE, Marakulin AV & Sholokhov EM (2010), All fiber er-tm q-switched laser. *Laser Physics Letters* 7, 795-797.

[5] Seguin F & Oleskevich TK (1993), Diode pumped q-switched fiber laser. *Optical Engineering* 32, 2036-2041.

[6] Lee GP & Newson TP (1996), Diode pumped high power simultaneously q-switched and self mode-locked erbium doped fiber laser. *Electronic Letters*, 32, 1685-1686.

[7] Richardson DJ, Nilsson J & Clarkson WA (2010), High power fiber lasers: current status and future perspectives. *Journal of Optical Society of America* 27, 63-92.

[8] Ahmad H, Hassan SNM, Ahmad F, Zulkifli MZ & Harun SW (2016), Broadband tuning in a passively q switched erbium doped fiber laser (edfl) via multiwall carbon nanotubes / polyvinyl alcohol (mwcnt/pva) saturable absorber. *Optics Communications* 365, 54-60.

[9] Hakulinen T & Okhotnikov OG (2007), 8 ns fiber laser q switched by the resonant saturable absorber mirror. *Optics Letters* 32, 2677-2679.

[10] Yamashita S, Inoue Y, Maruyama S, Murakami Y, Yaguchi H, Jablonski M & Set SY (2004), Saturable absorbers incorporating carbon nanotubes directly synthesized onto substrates and fibers and their application to mode-locked fiber lasers. *Optics Letters* 29, 1581-1583.

[11] Set S Y, Yaguchi H, Tanaka Y & Jablonski M (2004), Laser mode locking using a saturable absorber incorporating carbon nanotubes. *Journal of Lightwave Technology* 22, 51-56.

[12] Bao Q, Zhang H, Wang Y, Ni Z, Yan Y, Shen ZX, Loh KP & Tang DY (2009), Atomic-layer graphene as a saturable absorber for ultrafast pulsed lasers. *Advanced Functional Materials* 19, 3077-3083.

[13] Haris H, Harun SW, Muhammad AR, Anyi CL, Tan SJ, Ahmad F, Nor RM, Zulkepely NR & Arof H (2016), Passively q-switched erbium-doped and ytterbium-doped fibre lasers with topological insulator bismuth selenide (Bi_2Se_3) as saturable absorber. *Optics & Laser Technology* 88, 121-127.

[14] Yu Z, Song Y, Tian J, Dou Z, Guoyu H, Li K, Li H & Zhang X (2015), High-repetition-rate q-switched fiber laser with high quality topological insulator Bi_2Se_3 film. *Optics Express* 22, 11508-11515.

[15] Woodward R, Kelleher E, Howe R, Hu G, Torrisi F, Hasan T, Popov S & Taylor J (2014) Tunable q-switched fiber laser based on saturable edge-state absorption in few- layer molybdenum disulfide (MoS_2) *Optics Express* 22, 31113-311122.

[16] Ahmad H, Suthaskumar M, Tiu ZC, Zarei A & Harun SW (2016), Q-Switched erbium-doped fiber laser using $MoSe_2$ as saturable absorber. *Optics & Laser Technology* 79, 20-23.

[17] Li L, Wang Y, Fu Z, Wang X & Yang G (2017), High energy er-doped q-switched fiber laser with WS_2 saturable absorber *Optics Communications* 406, 80-84.

[18] Wang X, Luo Z, Liu H, Zhao M, Liu M, Zhu Y, Xue J, Luo A & Xu W (2015), Gold nanorod as saturable absorber for q-switched yb-doped fiber laser. *Optics Communications* 346, 21-25.

[19] Ahmad H, Ruslan NE, Ali ZA, Reduan SA, Lee CSJ, Shaharuddin RA, Nayan N & Ismail MA (2016), Ag-nanoparticle as a q switched device for tunable c-band fiber laser. *Optics Communications* 381, 85-90.

[20] Xu J-L, Li X-L, Wu Y-Z, Hao X-P, He J-L & Yang K-J (2011), Graphene saturable absorber mirror for ultra-fast-pulse solid-state laser. *Optics Letters* 36, 1948-1950.

[21] Gao C, Wang R, Zhu L, Gao M, Wang Q, Zhang Z, Wei Z, Lin J & Guo L (2012), Resonantly pumped 1.645 μm high repetition rate Er:YAG laser Q-switched by a graphene as a saturable absorber. *Optics Letters* 37, 632-634.

[22] Lagatsky AA, Sun Z, Kulmala TS, Sundaram RS, Milana S, Torrisi F, Antipov OL, Lee Y, Ahn JH, Brown CTA, Sibbett W & Ferrari AC (2013), 2 μm solid-state laser mode-locked by single-layer graphene. *Applied Physics Letters* 102, 013113.

[23] Liu J, Wu S, Yang Q-H & Wang P (2011), Stable nanosecond pulse generation from a graphene-based passively q-switched yb-doped fiber laser. *Optics Letters* 36, 4008-40010.

[24] Sobon G, Sotor J, Pasternak I, Grodecki K, Paletko P, Strupinski W, Jankiewicz Z & Abramski KM (2012), Er-doped fiber laser mode-locked by CVD-graphene saturable absorber. *Journal of Lightwave Technology* 30, 2770-2775.

[25] Zhang M, Kelleher EJR, Torrisi F, Sun Z, Hasan T, Popa D, Wang F, Ferrari AC, Popov SV & Taylor JR (2012), Tm-doped fiber laser mode-locked by graphene-polymer composite. *Optics Express* 20, 25077-25084.

[26] Sutter PW, Flege JI & Sutter EA (2008), Epitaxial graphene on ruthenium. *Nature Materials* 7, 406-411.

[27] Wang K, Tai G, Wong KH, Lau SP & Guo W (2011), Ni induced few layer graphene growth at low temperature by pulsed laser deposition. *AIP Advances* 1, 022141.

[28] Stankovich S, Dikin DA, Piner RD, Kohllhaas KA, Kleinhammes A, Jia Y, Wu Y, Nguyen ST & Ruoff RS (2007), Synthesis of graphene-based nanosheets via chemical reduction of exfoliated graphite oxide. *Carbon* 45, 1558-1565.

[29] Li X, Wang X, Zhang L, Lee S & Dai H (2008), Chemically derived, ultrasmooth graphene nanoribbon semiconductors. *Science* 319, 1229-1232.

[30] Liu N, Luo F, Wu H, Liu Y, Zhang C & Chen J (2008), One-step ionic liquid-assisted electrochemical synthesis of ionic-liquid-functionalized graphene sheets directly from graphite. *Advanced Functional Materials* 18, 1518-25.

[31] Lin GR & Lin YC (2011), Directly exfoliated and imprinted graphite nano-particle saturable absorber for passive mode-locking erbium doped fiber laser. *Laser Physics Letters* 8, 880-86.

[32] Lin YH & Lin GR (2012), Free-standing nano-scale graphite saturable absorber for passively mode-locked erbium doped fiber ring laser. *Laser Physics Letters* 9, 398-404.

[33] Lee J, Lee J, Koo J & Ju HL (2016), Graphite saturable absorber based on the pencil-sketching method for Q-switching of an erbium fiber laser. *Applied Optics* 55, 303-309.

[34] Yang C-Y, Wu C-L, Lin Y-H, Tsai L-H, Chi Y-C, Chang J-H, Wu C-I, Tsai H-K, Tsai D-P & Lin G-R (2013), Fabricating graphite nano-sheet powder by slow electrochemical exfoliation of large-scale graphite foil as a mode-locker for fiber lasers. *Optical Materials Express* 3, 1893-1905.

[35] Lin Y-H, Yang C-Y, Lin S-F & Lin G-R (2015), Triturating versatile carbon materials as saturable absorptive nano powders for ultrafast pulsating of erbium-doped fiber lasers. *Optical Materials Express* 5, 236-253.

[36] Bonaccorso F, Sun Z, Hasan T & Ferrari AC (2010), Graphene photonics and optoelectronics. *Nature Photonics* 4, 611-622.

[37] Liu Z-B, He X & Wang DN (2011), Passively mode-locked fiber laser based on a hollow-core photonic crystal fiber filled with few-layered graphene oxide solution. *Optics Letters* 36, 3024-3026.

[38] Xu J, Liu J, Wu S, Yang Q-H & Wang P (2012), Graphene oxide mode-locked femtosecond erbium-doped fiber lasers. *Optics Express* 20, 15474–15480.

[39] Jung M, Koo J, Park J, Song Y-W, Jhon YM, Lee K, Lee S & Lee JH (2013), Mode-locked pulse generation from an all-fiberized, Tm-Ho-codoped fiber laser incorporating a graphene oxide-deposited side-polished fiber. *Optics Express* 21, 20062-20072.

[40] Lee J, Koo J, Debnath P, Song Y-W & Lee JH (2013), A q-switched, mode-locked fiber laser using a graphene oxide-based polarization sensitive saturable absorber. *Laser Physics* Letters 10, 035103.

[41] Kobtsev S, Kukarin S & Fedotov Y (2008), Ultra-low repetition rate mode-locked fiber laser with high-energy pulses. *Optics Express* 16, 21936-21941.

[42] Ahmad H, Soltanian MRK, Narimani L, Amiri IS, Khodaei A & Harun SW (2015), Tunable s-band q-switched fiber laser using Bi_2Se_3 as the saturable absorber. *IEEE Photonics Journal* 7, 1502508.